ON THE CHOICE OF THE INITIAL CONDITIONS FOR DISPOSED SATELLITES OF GPS AND GALILEO CONSTELLATIONS

Diogo Merguizo Sanchez, sanchezfisica@gmail.com
Tadashi Yokoyama, tadashi@ms.rc.unesp.br
Pedro Ivo de Oliveira Brasil, pedro_brasil87@hotmail.com
Universidade Estadual Paulista (Unesp), Rio Claro – SP, Brasil
Ricardo Reis Cordeiro, cordeiro@ufv.br
Universidade Federal de Viçosa, Viçosa – MG, Brasil

Abstract. *Through the averaged equations we revisit theoretical and numerical aspects of the strong resonance that increases the eccentricity and affects the stability of the disposed objects of GPS and Galileo Systems. A simple view of the phase space shows that the resonance that causes this increase does not depend on the semi-major axis of the disposed object. This is easily identified considering a simple expansion of the disturbing function, where the Sun can be assumed in circular orbit. Here we also present a complete expansion of first order in the eccentricity of the Sun. Since the resonance does not depend on the altitude of the satellite, usual strategies of changing semi-major axes (raising perigee), do not solve the problem. Following Gick and Chao (2001), in this work we search for a set of initial conditions such that the deactivated satellites or upper-stages remain at least for 250 years without penetrating in the orbits of the operational satellites of the constellation. In the case that Moon's perturbation is not significant, we can identify, very clearly in the phase space, the regions where eccentricity reaches maximum and minimum values so that any risk of collision can be avoided. Based on this, we numerically found the (ω, Ω) values that keep decommissioned objects for at least 250 years. In particular, for the GALILEO case, the theoretical results predicted in the averaged system are in good agreement with numerical results. The initial inclination of the Moon's orbit shows interesting differences.*

***Keywords**: Galileo-GPS system, resonance, space debris.*

1. INTRODUCTION

Broadly speaking, the GPS, GLONASS and GALILEO systems are satellite constellations which were designed mainly for positioning and navigation purposes. The first members of GPS (block I), originally were designed to have inclination of 63.4 degrees with respect to the equator, distributed in three orbital planes, each one separated from 120 degrees in the longitude of the node. The altitude is 20,200 km. The GLONASS members are similar, with slightly lower altitude (19,100 km, period = 11:15 h). The European GALILEO system is still in construction, and the inclination of the satellites will be 55, 56 degrees, with altitude 23,615 km. All the three systems have rather similar altitudes. In order to avoid risks of collision and following American Govern instructions about debris mitigation, there are some recommendations that the disposal satellites and upper-stages should be deposited at least 500 km above or below the semi-synchronous orbit.

In a constellation of a navigation system, the members must be kept under precise requirements of functionality. However after some time, they have to be deactivated, since some level of these requirements cannot be fulfilled for long time. The destination of these deactivated objects is a problem, since they must be moved into some disposal regions in order to preclude collisions with operational members of the constellation. While these vehicles can be designed "a priori" to transport additional propellant (at some non-negligible cost) to be used in some planned maneuvers to insert them in the disposal regions, the same is not true for the upper-stage. In some cases (block IIF of GPS system), due to design restrictions, this upper-stage cannot be easily guided to the disposal region. It must perform several operations after the satellite is injected in the constellation. All these operations change its final parameters, Jenkin and Gick (2006). Since the inclination of these vehicles are near to 55-56 degrees, the eccentricity, suffer strong variations and even an initially circular orbit, can become highly eccentric, so that they can cross very easily the orbit of the operational satellites. What is interesting and also problematic is the fact that the rate of growing the eccentricity is very sensitive to the initial parameters of the disposal orbit (eccentricity, argument of the perigee, and longitude of the node). In this work, based on the theoretical framework, we present a set of initial conditions (ω, Ω) for GPS and GALILEO systems such that the disposed objects can remain at the least 250 years with small eccentricity (0.01 or 0.02) without causing any risk to the operational satellites.

The above strategy of keeping small eccentricity can generate some additional problem: after some time, the disposed vehicles will accumulate and a graveyard of these objects will be created. Therefore, a risk of collisions amongst themselves is a crucial problem, since the products of these extra collisions are almost untrackable fragments that may offer more risks to the operational elements of the constellation.

According to Jenkin and Gick (2005), the strategy in the opposite direction, that is, exploiting the growth of the eccentricity in order to diluting disposal orbit collision risk, has some interesting points to be considered: the percentage of disposed vehicles that will re-enter in the atmosphere can be increased. Another advantage observed is: although eccentricity growth strategy increases the collision risk in the constellation, in some cases this risk can be reversed with proper choice of the initial disposal eccentricity.

In this sense, we also started the investigation of some initial conditions that can cause large increase of the eccentricity, for a minimum time interval, considering different initial inclination of the Moon's orbit.

2. METHODS

2.1. Disturbing Function of the Sun

As we want to highlight some theoretical aspects, it is instructive to write the main disturbing forces in terms of the orbital elements.

In this section we obtain the averaged disturbing function of the Sun. Following the classical procedure, Brouwer and Clemence (1961), in a reference center fixed in the Earth equator, the disturbing function of the Sun is:

$$R_\odot = k^2 M_\odot \left(\frac{1}{|\vec{r} - \vec{r}_\odot|} - \frac{\vec{r}\cdot\vec{r}_\odot}{|\vec{r}_\odot|^3} \right), \tag{1}$$

where $M_\odot$ is the mass of the Sun, k^2 is the gravitational constant, $\vec{r}$, $\vec{r}_\odot$ are position vector of the satellite and the Sun respectively.

Expanding Eq. (1) in powers of $(\vec{r}/\vec{r}_\odot)$ up to order 2 we have:

$$R_\odot = \frac{k^2 M_\odot a^2}{r_\odot^3} \left(\frac{r^2}{a^2} \right) \left(-\frac{1}{2} + \frac{3}{2} \cos^2(S) \right). \tag{2}$$

S is the angular distance between the satellite and the Sun. We use the classical notation: *a, e, I, l,* ω, *Ω*, for semi-major axis, eccentricity, inclination, argument of the perigee and longitude of the node. The same set is used for the Sun's elements, adding the index ⊙.

For the moment we consider Sun in a circular orbit. From the geometry of the problem, and using classical relations of the two body problem we get:

$$\begin{aligned} \cos(S) = &\tfrac{1}{4}(1+\cos(I))(1-\cos(I_\odot))\cos(f+\omega+f_\odot+\omega_\odot+\Omega-\Omega_\odot) \\ &+\tfrac{1}{4}(1-\cos(I))(1+\cos(I_\odot))\cos(f+\omega+f_\odot+\omega_\odot-\Omega+\Omega_\odot) \\ &+\tfrac{1}{4}(1+\cos(I))(1+\cos(I_\odot))\cos(f+\omega-f_\odot-\omega_\odot+\Omega-\Omega_\odot) \\ &+\tfrac{1}{4}(1-\cos(I))(1-\cos(I_\odot))\cos(f+\omega-f_\odot-\omega_\odot-\Omega+\Omega_\odot) \\ &+\tfrac{1}{2}\sin(I)\sin(I_\odot)\left[\cos(f+\omega-f_\odot-\omega_\odot)-\cos(f+\omega+f_\odot+\omega_\odot)\right], \end{aligned} \tag{3}$$

or in a compact form:

$$\cos(S) = Aa + Bb + Cc + Dd + Ee, \tag{4}$$

where: $A = \frac{1}{4}(1+\cos(I))(1-\cos(I_\odot))$;

$a = \cos(f+\omega+f_\odot+\omega_\odot+\Omega-\Omega_\odot)$;

$B = \frac{1}{4}(1-\cos(I))(1+\cos(I_\odot))$;

$b = \cos(f+\omega+f_\odot+\omega_\odot-\Omega+\Omega_\odot)$;

$C = \frac{1}{4}(1+\cos(I))(1+\cos(I_\odot))$;

$c = \cos(f+\omega-f_\odot-\omega_\odot+\Omega-\Omega_\odot)$;

$D = \frac{1}{4}(1-\cos(I))(1-\cos(I_\odot))$;

$d = \cos(f+\omega-f_\odot-\omega_\odot-\Omega+\Omega_\odot)$;

$E = \frac{1}{2}\sin(I)\sin(I_\odot)$;

$e = \cos(f+\omega-f_\odot-\omega_\odot)-\cos(f+\omega+f_\odot+\omega_\odot)$;

f, $f_\odot$: true anomaly of the satellite and of the Sun.

The average is obtained from

$$\langle R_\odot \rangle = \frac{1}{2\pi}\int_0^{2\pi} R_\odot dl \tag{5}$$

$$\begin{aligned}
R_\odot^* = \langle R_\odot \rangle = \frac{k^2 M_\odot a^2}{2 r_\odot^3}\Big[& \frac{3}{2} P \left(A^2 + B^2 + C^2 + D^2 + 2E^2 - \frac{2}{3}\right) \\
& + \frac{3}{2} A^2 Z cos(2\omega + 2f_\odot + 2\omega_\odot + 2\Omega - 2\Omega_\odot) \\
& + \frac{3}{2} B^2 Z cos(2\omega + 2f_\odot + 2\omega_\odot - 2\Omega + 2\Omega_\odot) \\
& + \frac{3}{2} C^2 Z cos(2\omega - 2f_\odot - 2\omega_\odot + 2\Omega - 2\Omega_\odot) \\
& + \frac{3}{2} D^2 Z cos(2\omega - 2f_\odot - 2\omega_\odot - 2\Omega + 2\Omega_\odot) \\
& + \frac{3}{2} Z(E^2 + 2CD) cos(2\omega - 2f_\odot - 2\omega_\odot) \\
& + \frac{3}{2} Z(E^2 + 2AB) cos(2\omega + 2f_\odot + 2\omega_\odot) \\
& + 3Z(-E^2 + AD + BC) cos(2\omega) \\
& + 3P(-E^2 + AC + BD) cos(2f_\odot + 2\omega_\odot) \\
& + 3P(AB + CD) cos(2\Omega - 2\Omega_\odot) \\
& + 3ACZ cos(2\omega + 2\Omega - 2\Omega_\odot) \\
& + 3ADP cos(2f_\odot + 2\omega_\odot + 2\Omega - 2\Omega_\odot) \\
& + 3EP(A - D) cos(2f_\odot + 2\omega_\odot + \Omega - \Omega_\odot) \\
& + 3EP(-A - B + C + D) cos(\Omega - \Omega_\odot) \\
& + 3EZ(A - C) cos(2\omega + \Omega - \Omega_\odot) \\
& - 3AEZ cos(2\omega + 2f_\odot + 2\omega_\odot + \Omega - \Omega_\odot) \\
& + 3BCP cos(2f_\odot + 2\omega_\odot - 2\Omega + 2\Omega_\odot) \\
& + 3BDZ cos(2\omega - 2\Omega + 2\Omega_\odot) \\
& + 3EP(B - C) cos(2f_\odot + 2\omega_\odot - \Omega + \Omega_\odot) \\
& + 3EZ(B - D) cos(2\omega - \Omega + \Omega_\odot) \\
& - 3BEZ cos(2f_\odot + 2\omega + 2\omega_\odot - \Omega + \Omega_\odot) \\
& + 3CEZ cos(2\omega - 2f_\odot - 2\omega_\odot + \Omega - \Omega_\odot) \\
& + 3DEZ cos(2\omega - 2f_\odot - 2\omega_\odot - \Omega + \Omega_\odot)\Big],
\end{aligned} \tag{6}$$

where $P = 1 + \frac{3}{2}e^2$, $Z = \frac{5}{2}e^2$.

After a second and similar average with respect to the mean anomaly of the Sun, we get:

$$\begin{aligned}
\hat{R}_\odot = \frac{k^2 M_\odot a^2}{4 r_\odot^3}\Big[& \frac{P}{4}\left(1 - 3cos^2(I) - 3cos^2(I_\odot) + 9cos^2(I)cos^2(I_\odot)\right) \\
& + \frac{3}{2} Z sin^2(I) \left(-1 + 3cos^2(I_\odot)\right) cos(2\omega) \\
& + \frac{3}{2} P sin^2(I) sin^2(I_\odot) cos(2\Omega - 2\Omega_\odot) \\
& + \frac{3}{8} Z\big(1 + cos(I)\big)^2 sin^2(I_\odot) cos(2\omega + 2\Omega - 2\Omega_\odot) \\
& - \frac{3}{2} Z sin(I) sin(I_\odot)\big(1 + cos(I)\big) cos(I_\odot) cos(2\omega + \Omega - \Omega_\odot) \\
& + 3P sin(I) cos(I) sin(I_\odot) cos(I_\odot) cos(\Omega - \Omega_\odot) \\
& + \frac{3}{8} Z\big(1 + cos^2(I)\big)^2 sin^2(I_\odot) cos(2\omega - 2\Omega + 2\Omega_\odot) \\
& + \frac{3}{2} Z sin(I)\big(1 - cos(I)\big) sin(I_\odot)\, cos(I_\odot)\, cos(2\omega - \Omega + \Omega_\odot)\Big].
\end{aligned} \tag{7}$$

2.2. Oblateness Disturbing Function

For the oblateness, we have:

$$U_2 = \frac{k^2 M_T R_P^2}{r^3} J_2 \left(\frac{1}{2} - \frac{3}{2} sin^2(\beta)\right) \tag{8}$$

where R_P, J_2 and β are: equatorial radius of the planet, oblateness coefficient and latitude of the satellite, respectively.
The average with respect to the mean anomaly of the satellite gives:

$$R_{J_2} = \langle U_2 \rangle = \frac{1}{4} n^2 J_2 R_P^2 (3cos^2(I) - 1)(1 - e^2)^{-\frac{3}{2}}, \tag{9}$$

where n is the mean motion of the satellite.

2.3. Equations of the motion

Therefore the averaged equations are given through the disturbing function:

$$R = \hat{R}_\odot + R_{J_2} \tag{10}$$

The equations for the osculating elements (exact system), including Moon are:

$$\ddot{\vec{r}} = -\frac{k^2(M+m)}{r^3}\vec{r} - k^2 M_\odot \left(\frac{\vec{r}-\vec{r}_\odot}{|\vec{r}-\vec{r}_\odot|^3} - \frac{\vec{r}_\odot}{|\vec{r}_\odot|^3}\right) - k^2 M_L \left(\frac{\vec{r}-\vec{r}_L}{|\vec{r}-\vec{r}_L|^3} - \frac{\vec{r}_L}{|\vec{r}_L|^3}\right) + \vec{P}_{J_2}, \tag{11}$$

$$P_{J_x} = -k^2 M J_2 R_P^2 \left[\frac{3x}{2r^5} - \frac{15}{2}\frac{z^2 x}{r^7}\right], \tag{12}$$

$$P_{J_y} = -k^2 M J_2 R_P^2 \left[\frac{3y}{2r^5} - \frac{15}{2}\frac{z^2 y}{r^7}\right], \tag{13}$$

$$P_{J_z} = -k^2 M J_2 R_P^2 \left[\frac{9z}{2r^5} - \frac{15}{2}\frac{z^3}{r^7}\right], \tag{14}$$

where the components of $\vec{P}_{J_2}$ are: P_{J_x}, P_{J_y}, P_{J_z} and M, m, M_L are the masses of the planet, satellite and Moon and $\vec{r}$, $\vec{r}_\odot$ and $\vec{r}_L$ are the position vector of the satellite, Sun and Moon respectively.

2.4. Some special resonances

For close satellites, usually the oblateness is the dominant part. In this case, the main frequencies of the system are given by:

$$\dot{\omega} \approx \frac{3nJ_2R_P^2}{4a^2(1-e^2)^2}(5cos^2(I) - 1), \tag{15}$$

$$\dot{\Omega} \approx -\frac{3nJ_2R_P^2}{2a^2(1-e^2)^2} cos(I). \tag{16}$$

The ratio of these two frequencies is:

$$\frac{\dot{\Omega}}{\dot{\omega}} \approx \frac{2cos(I)}{1-5cos^2(I)} = k. \tag{17}$$

Note that for k = integer we have the special resonances which do not depend on the semi-major axis. These resonances usually affect the eccentricity. For $k = -2$ we have $2\dot{\omega} + \dot{\Omega} \approx 0$ for I = 56.06° and I = 110.99°. For I = 63.4°, we have $\dot{\omega} \approx 0$.

3. EFFECTS OF $2\dot{\omega}+\dot{\Omega}$ AND $\dot{\omega}$ RESONANCES

For the moment let us consider only $R^*_\odot + R_{J_2}$: Fig. 1 and Fig. 2, show the effects of both resonances on the eccentricity and on the resonant angles. Note that an initial small eccentricity reaches a significant increase.

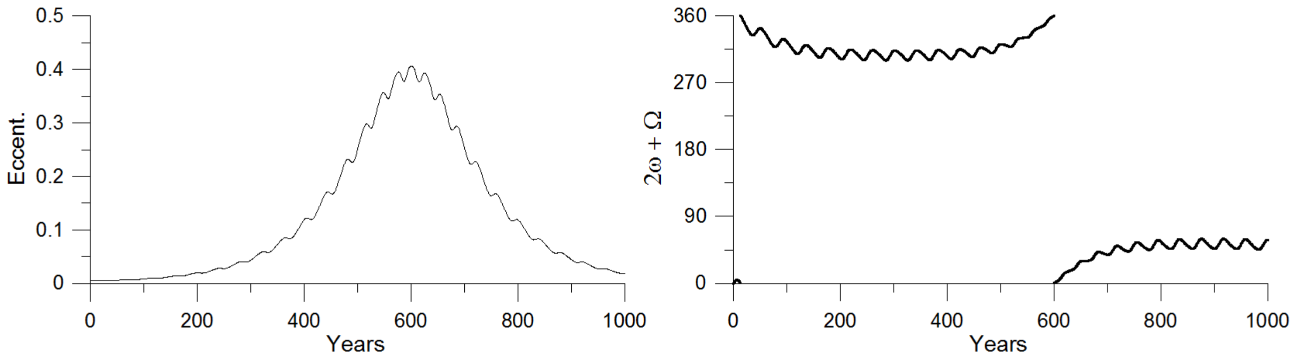

Figure 1. Time evolution of the eccentricity (left) and the critical angle (right). Initial conditions: a = 4.805 R_T (30,647 km), e = 0.005, I = 56.06° and other elements equal to zero.

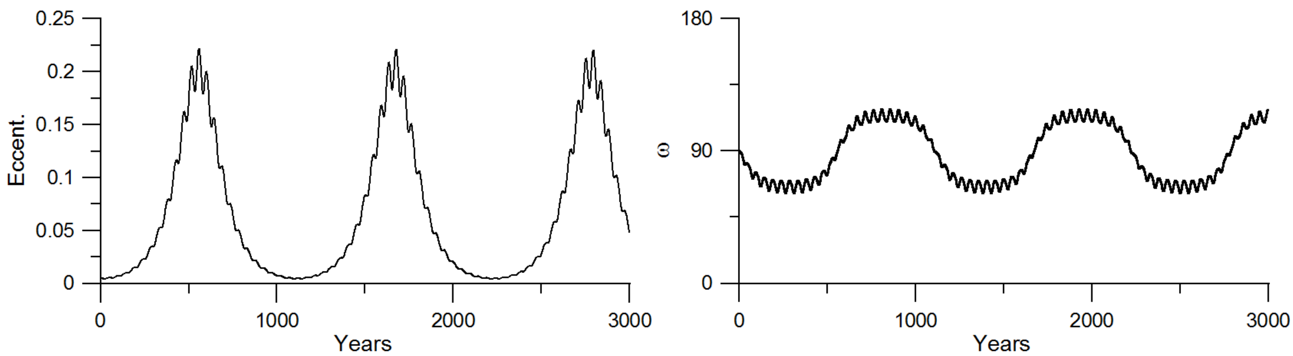

Figure 2. Time evolution of the eccentricity (left) and the critical angle (right). Initial conditions: a = 4.7 R_T (≈ 29,977 km), e = 0.005, I = 63.4° and other elements equal to zero.

Let us pay more attention to the case I = 56.06° which is the inclination of the members of the Galileo constellation. For this inclination the dominant term in the $R^*_\odot$ is $cos(2\omega+\Omega-\Omega_\odot)$. Neglecting the remaining terms of $R^*_\odot$, the Hamiltonian of the problem is:

$$F = R_{J_2} + \frac{k^2 M_\odot a^2}{2r_\odot^3}\Bigg[\frac{P}{8}\Big(1-3cos^2(I)-3cos^2(I_\odot)+9cos^2(I)cos^2(I_\odot)\Big) -\frac{3}{4}Zsin(I)sin(I_\odot)\big(1+cos(I)\big)cos(I_\odot)cos(2\omega+\Omega-\Omega_\odot)\Bigg], \quad (18)$$

Let us take $L=\sqrt{k^2(M_T+m)a}$, $G=L\sqrt{1-e^2}$, $H=Gcos(I)$, l, ω, Ω the set of the Delaunay variables with ω, Ω instead g, h. After a trivial Mathieu canonical transformation, Lanczos (1970):

$$\theta_1 = 2\omega+\Omega,\ P_1=\frac{G}{2},\ \theta_2=h,\ P_2=H-\frac{G}{2}, \quad (19)$$

then we have:

$$\tilde{R}_\odot = \frac{k^2 M_\odot a^2}{2r_\odot^3}\Bigg[\frac{P}{8}\left(1-3\frac{(P_1+P_2)^2}{4P_1^2}-3cos^2(I_\odot)+9\frac{(P_1+P_2)^2}{4P_1^2}cos^2(I_\odot)\right) -\frac{3}{4}Z\left(1-\frac{(P_1+P_2)^2}{4P_1^2}\right)^{\frac{1}{2}}sin(I_\odot)\left(1+\frac{P_1+P_2}{2P_1}\right)cos(I_\odot)cos(\theta_1)\Bigg], \quad (20)$$

$$\tilde{R}_{J_2} = \frac{1}{4} n^2 J_2 R_P^2 \left(3 \frac{(P_1+P_2)^2}{4P_1^2} - 1\right) \left(1 - \frac{L^2-4P_1^2}{L^2}\right)^{-\frac{3}{2}}. \tag{21}$$

In these variables, this is a one degree of freedom problem, whose dynamics is very similar to the very well known Lidov-Kozai resonance. In Fig. 3, we consider an initial eccentricity e_0 = 0.005 and semi-major axis a = 4.805 R_T (30,647 km). This figure is very instructive: note that in the bottom part there is a large region where the satellite remains some finite time with very small eccentricity. These are the exactly region we are looking for. It corresponds to the region where $2\omega + \Omega \approx 0$. On the other hand, we have the counterpart of this situation at the top of the figure: very high eccentricity, which occurs again for $2\omega + \Omega \approx 0$. We can separate these two configurations and have a clear view of these two cases. Only to confirm our reasoning, let us integrate the problem in Cartesian coordinates, using Eq. (11). We also have to decrease the effect of the Moon's perturbation since in this analysis we considered only $\tilde{R}_{\odot}$ and $\tilde{R}_{J_2}$. To do that, we consider convenient value for the semi-major axis. Figure 4 (initial conditions: a = 3.5 R_T ($\approx$ 22323 km), e = 0.005, I = 56.06° and other elements equal to zero; Moon inclination I_L = 18.28) shows clearly that the minimum of eccentricity occurs when $2\omega + \Omega \approx 0$ is crossed in the descendent direction, while maximum occurs for increasing direction. It is worth noting that if the semi-major axis is high, then the effect of the Moon cannot be neglected, so that the problem is no more a one degree of freedom problem. In this case the search of the (ω, Ω) pair such that eccentricity remains small, must be done integrating the complete equations of the motion as given in Eq. (11).

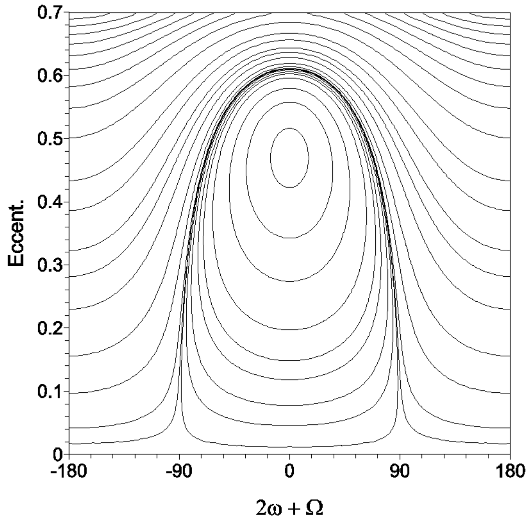

Figure 3. Level curves of Hamiltonian, showing the eccentricity variation vs. resonant angle.

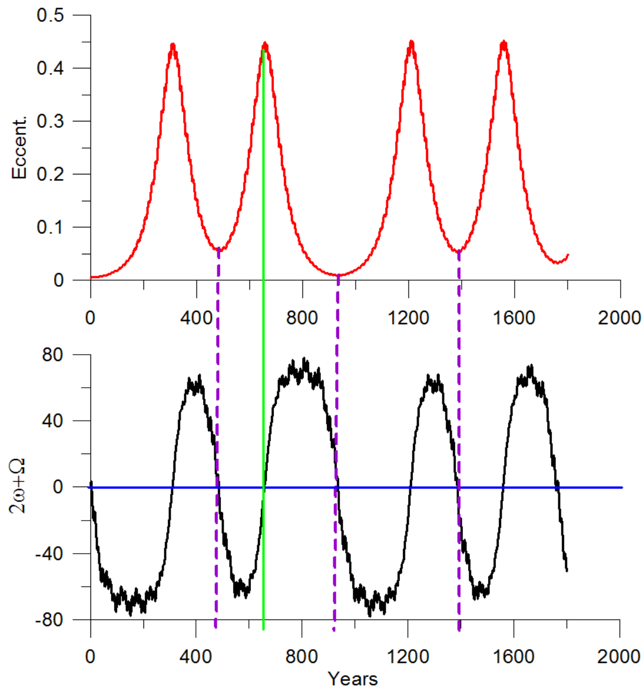

Figure 4. Time evolution of the eccentricity (top) and the critical angle (bottom) for a disposal GPS satellite. Note that the minimum of the eccentricity occurs when $2\omega + \Omega$ is crossing zero in descendent direction while maximum occurs when $2\omega + \Omega$ is crossing zero, but in increasing direction.

3. (ω, Ω) CONDITIONS FOR GALILEO CASE

In this section we integrate the osculating elements of a disposal satellite of the Galileo system under the effect of the Sun, Moon and the oblateness. As we said before, we take 500 km above of the nominal altitude of the constellation. The initial elements are fixed to a = 4.805R_T (30,647 km), e = 0.005, l = 0° and I = 56.06°. We consider two cases for the Moon's inclination I = 18.28° and 28.58°. We show that the initial value of the inclination is important as shown in Figs. 5 and 6. In these figures we show the pair (ω, Ω) such that the disposal object remains at least 250 years with eccentricity smaller than 0.01, so that there is no risk of collision with any member of the constellation. The black region corresponds to initial conditions such that the satellite remains at least 250 years with maximum eccentricity less than 0.01. In the green region the maximum eccentricity is less than 0.02. The two straight lines represent the exact condition $2\omega + \Omega = k\pi$ (in particular we only plot the case k = 0). Note that, in special, the black dots (Fig. 5) are formed in the places predicted form the previous theoretical model. For the remain figures, the black dots are slightly shifted (upward) from the line $2\omega + \Omega = 0$. We believe that this is caused by the strong perturbation of the Moon. Fig. 7 shows the time evolution of the eccentricity for integration whose initial conditions are obtained from Fig. 5 (small square in the bottom). As expected, the eccentricity remains very low, while if we take (ω, Ω) outside the marked regions in Fig. 5 or 6, a significant increase is verified as shown in Fig. 8. The initial (ω, Ω) used in this case correspond to the star given in Fig. 5.

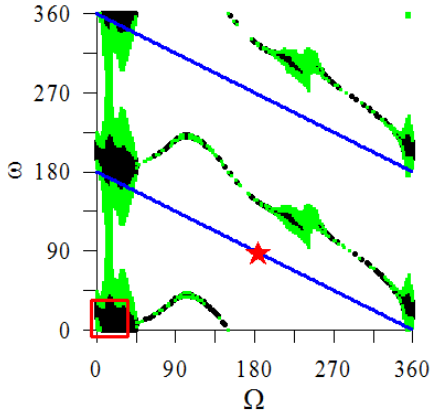

Figure 5. Black dots: represent (ω, Ω) values such that a satellite with a = 30,647 km remains at least 250 years with $e_{MAX} \leq 0.01$. Green dots: the same, but $e_{MAX} \leq 0.02$. Blue dots: curve satisfying $2\omega + \Omega = 0$. Moon's inclination: I_L = 18.28°. Note that most of the "stable" (black dots) (ω, Ω) points satisfy $2\omega + \Omega = 0, 2\pi$ with $\Omega \approx 0$, $\omega = \pi$.

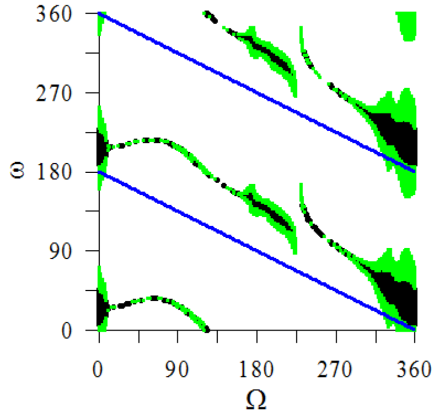

Figure 6. Same of Fig. 5, but now I_L = 28.58°.

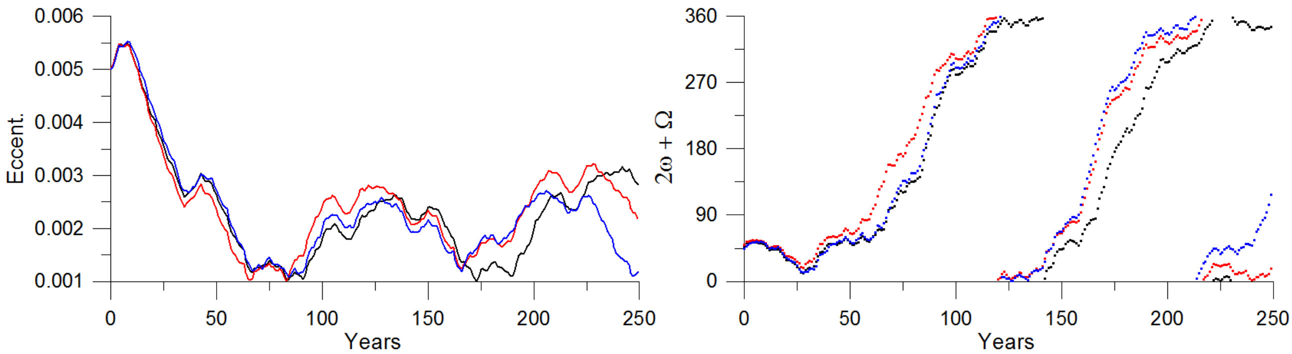

Figure 7. Time evolution of the eccentricity (left) and the critical angle (right). Initial conditions: a = 4.805 R_T, e = 0.005, I = 56.06°. Initial (ω, Ω): (24°, 0°) – black, (23°, 2°) – red, (18°, 8°) – blue. These initial conditions were extracted from the red square shown in Fig. 5. I_L = 18.28°.

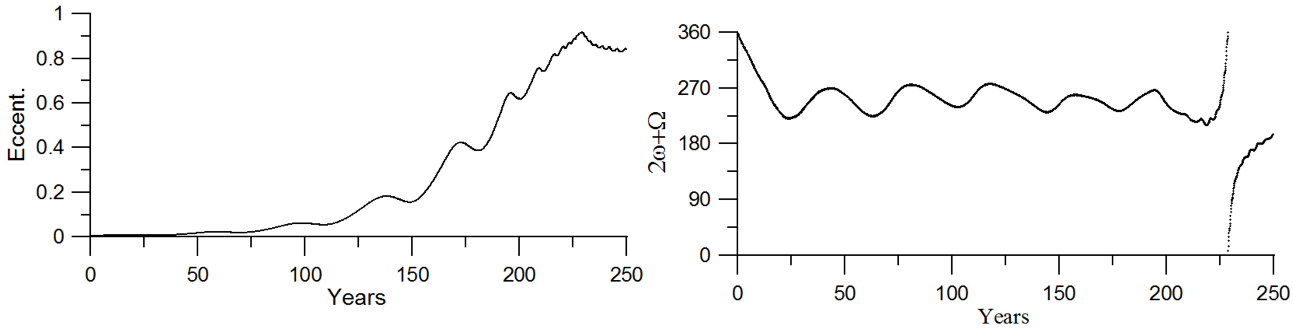

Figure 8. The time evolution of the eccentricity (left) and the critical angle (right). Initial conditions: a = 4.805 R_T (30,647 km), e = 0.005, I = 56.06°, ω = 90°, Ω = 180°. This initial condition is marked by red star in Fig. 5.

4. (ω, Ω) CONDITIONS FOR GPS CASE

This time we consider the GPS system. Again we consider I = 18.28 and I = 28.58 for the Moon's inclination. As before the importance of the Moon's inclination is very clear.

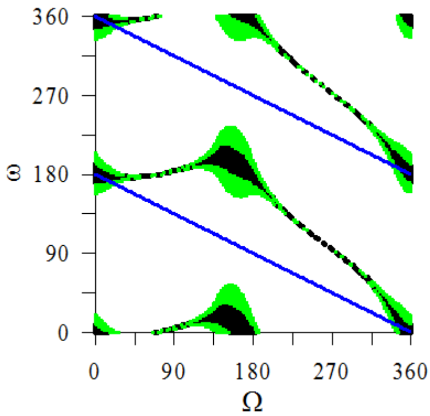

Figure 9. Same of Fig. 5, but now a = 26,060 km.

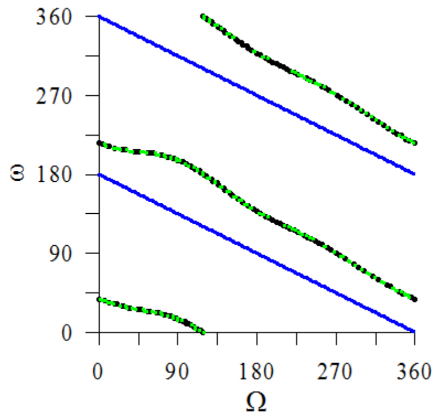

Figure 10. Same of Fig. 9, but now I_L = 28.58°.

5. CONCLUSION

With the averaged equations we clearly showed the dynamics of the $2\omega + \Omega$ resonance. The reason of the increase of the eccentricity is essentially due to this resonance which does not depend on the value of the semi-major axis. Therefore, any change of the semi-major axes (raising the perigee) of the decommissioned object will not remove from the resonance. After showing the existence of some initial conditions in the (ω, Ω) domain where the eccentricity can remain very small for a simplified model, we used the complete set of equations to search this pair in (ω, Ω) plane. The importance of the Moon's inclination becomes very clear as shown in Figs. 5, 6, 9, 10. We obtained these initial values for GALILEO and GPS systems. For completeness, we also derived a first order averaged system in the eccentricity of the third body. Several additional resonances appear although their effect seems to be not so relevant for the navigation system. The search of the (ω, Ω) pair for the maximum increase of the eccentricity can be done very easily following the same procedure we used for small eccentricity. For completeness, in the disturbing function of the geopotential we also investigated the contribution of terms coming from J_{22}, J_{32} and J_{33}. We intend to show the corresponding Figures 9 and 10 in a separated paper including the second strategy of exploiting the increase the eccentricity.

6. ACKNOWLEDGEMENTS

The authors thank CNPQ, FAPESP and FUNDUNESP.

7. REFERENCES

Brouwer, D. and Clemence, G., 1961, "Methods of Celestial Mechanics". Academic Press, New York.
Gick, R.A. and Chao, C.C., 2001, "GPS Disposal Orbit Stability and Sensitivity Study", Advances in the Astronomical Sciences, vol.108, pp. 2005-2018.
Jenkin, A.B. and Gick, R.A., 2005, "Dilution of Disposal Orbit Collision for the Medium Earth Orbit Constellations",

The Astron. Journal 126, pp. 398-429.

Jenkin, A.B. and Gick, R.A., 2006, "Collision Risk Posed to the Global Positioning System by Disposed Upper Stages". Journal of Spacecraft and Rockets vol.43, No. 6, pp. 1412-1418.

Lanczos, C., 1970, "The Variational Principles of Mechanics". Fourth Edition – Univ. Toronto Press.

Rossi, A., 2008, "Resonant dynamics of Medium Earth Orbits: space debris issues". Celestial Mechanics and Dynamical Astronomy, Volume 100, Issue 4, pp.267-286.

Yokoyama, T., 1999, "Dynamics of some fictitious satellite of Venus and Mars". Planetary and Space Science, vol. 47, Issue 1, pp. 619-627.

Yokoyama, T., 2002, "Possible effects of secular resonances in Phobos and Triton", Planetary and Space Science, vol. 50, Issue 1, pp. 63-77.

8. RESPONSIBILITY NOTICE

The authors are the only responsible for the material included in this paper.

9. APPENDIX

Here we give the complete expression of the averaged disturbing function up to first order in eccentricity of the third body.

$$
\begin{aligned}
R_{\odot}^{1} = \frac{k^2 M_{\odot}^3 a^3}{2a_{\odot}^3} e_{\odot} \Big[& \frac{9}{2} P\left(A^2+B^2+C^2+D^2+2E^2-\frac{2}{3}\right)\cos\, l_{\odot} \\
& + \frac{9}{4} A^2 Z cos(2\omega + l_{\odot} + 2\omega_{\odot} + 2\Omega - 2\Omega_{\odot}) \\
& + \frac{9}{4} A^2 Z cos(2\omega + 3l_{\odot} + 2\omega_{\odot} + 2\Omega - 2\Omega_{\odot}) \\
& + \frac{9}{4} B^2 Z cos(2\omega + l_{\odot} + 2\omega_{\odot} - 2\Omega + 2\Omega_{\odot}) \\
& + \frac{9}{4} B^2 Z cos(2\omega + 3l_{\odot} + 2\omega_{\odot} - 2\Omega + 2\Omega_{\odot}) \\
& + \frac{9}{4} C^2 Z cos(2\omega - 3l_{\odot} - 2\omega_{\odot} + 2\Omega - 2\Omega_{\odot}) \\
& + \frac{9}{4} C^2 Z cos(2\omega - l_{\odot} - 2\omega_{\odot} + 2\Omega - 2\Omega_{\odot}) \\
& + \frac{9}{4} D^2 Z cos(2\omega - 3l_{\odot} - 2\omega_{\odot} - 2\Omega + 2\Omega_{\odot}) \\
& + \frac{9}{4} D^2 Z cos(2\omega - l_{\odot} - 2\omega_{\odot} - 2\Omega + 2\Omega_{\odot}) \\
& + \frac{9}{4} Z(E^2 + 2CD) cos(2\omega - 3l_{\odot} - 2\omega_{\odot}) \\
& + \frac{9}{4} Z(E^2 + 2CD) cos(2\omega - l_{\odot} - 2\omega_{\odot}) \\
& + \frac{9}{4} Z(E^2 + 2AB) cos(2\omega + l_{\odot} + 2\omega_{\odot}) \\
& + \frac{9}{4} Z(E^2 + 2AB) cos(2\omega + 3l_{\odot} + 2\omega_{\odot}) \\
& + \frac{9}{2} Z(-E^2 + AD + BC) cos(l_{\odot} - 2\omega) \\
& + \frac{9}{2} Z(-E^2 + AD + BC) cos(l_{\odot} + 2\omega) \\
& + \frac{9}{2} P(-E^2 + AC + BD) cos(l_{\odot} + 2\omega_{\odot}) \\
& + \frac{9}{2} P(-E^2 + AC + BD) cos(3l_{\odot} + 2\omega_{\odot}) \\
& + \frac{9}{2} P(AB + CD) cos(l_{\odot} - 2\Omega + 2\Omega_{\odot}) \\
& + \frac{9}{2} P(AB + CD) cos(l_{\odot} + 2\Omega - 2\Omega_{\odot}) \\
& + \frac{9}{2} ACZ cos(l_{\odot} - 2\omega - 2\Omega + 2\Omega_{\odot})
\end{aligned}
$$

$$+\frac{9}{2}ACZcos(l_{\odot}+2\omega+2\Omega-2\Omega_{\odot})$$
$$+\frac{9}{2}ADPcos(l_{\odot}+2\omega_{\odot}+2\Omega-2\Omega_{\odot})$$
$$+\frac{9}{2}ADPcos(3l_{\odot}+2\omega_{\odot}+2\Omega-2\Omega_{\odot})$$
$$+\frac{9}{2}EP(A-D)cos(l_{\odot}+2\omega_{\odot}+\Omega-\Omega_{\odot})$$
$$+\frac{9}{2}EP(A-D)cos(3l_{\odot}+2\omega_{\odot}+\Omega-\Omega_{\odot})$$
$$+\frac{9}{2}EP(-A-B+C+D)cos(l_{\odot}-\Omega+\Omega_{\odot})$$
$$+\frac{9}{2}EP(-A-B+C+D)cos(l_{\odot}+\Omega-\Omega_{\odot})$$
$$+\frac{9}{2}EZ(A-C)cos(l_{\odot}-2\omega-\Omega+\Omega_{\odot})$$
$$+\frac{9}{2}EZ(A-C)cos(l_{\odot}+2\omega+\Omega-\Omega_{\odot})$$
$$-\frac{9}{2}AEZcos(2\omega+l_{\odot}+2\omega_{\odot}+\Omega-\Omega_{\odot})$$
$$-\frac{9}{2}AEZcos(2\omega+3l_{\odot}+2\omega_{\odot}+\Omega-\Omega_{\odot})$$
$$+\frac{9}{2}BCPcos(l_{\odot}+2\omega_{\odot}-2\Omega+2\Omega_{\odot})$$
$$+\frac{9}{2}BCPcos(3l_{\odot}+2\omega_{\odot}-2\Omega+2\Omega_{\odot})$$
$$+\frac{9}{2}BDZcos(l_{\odot}-2\omega+2\Omega-2\Omega_{\odot})$$
$$+\frac{9}{2}BDZcos(l_{\odot}+2\omega-2\Omega+2\Omega_{\odot})$$
$$+\frac{9}{2}EP(B-C)cos(l_{\odot}+2\omega_{\odot}-\Omega+\Omega_{\odot})$$
$$+\frac{9}{2}EP(B-C)cos(3l_{\odot}+2\omega_{\odot}-\Omega+\Omega_{\odot})$$
$$+\frac{9}{2}EZ(B-D)cos(l_{\odot}-2\omega+\Omega-\Omega_{\odot})$$
$$+\frac{9}{2}EZ(B-D)cos(l_{\odot}+2\omega-\Omega+\Omega_{\odot})$$
$$-\frac{9}{2}BEZcos(l_{\odot}+2\omega+2\omega_{\odot}-\Omega+\Omega_{\odot})$$
$$-\frac{9}{2}BEZcos(3l_{\odot}+2\omega+2\omega_{\odot}-\Omega+\Omega_{\odot})$$
$$+\frac{9}{2}CEZcos(2\omega-3\,l_{\odot}-2\omega_{\odot}+\Omega-\Omega_{\odot})$$
$$+\frac{9}{2}CEZcos(2\omega-\,l_{\odot}-2\omega_{\odot}+\Omega-\Omega_{\odot})$$
$$+\frac{9}{2}DEZcos(2\omega-3\,l_{\odot}-2\omega_{\odot}-\Omega+\Omega_{\odot})$$
$$+\frac{9}{2}DEZcos(2\omega-\,l_{\odot}-2\omega_{\odot}-\Omega+\Omega_{\odot})]$$